Radiotherapy and Oncology 141 (2019) 227–233

Contents lists available at ScienceDirect

Radiotherapy and Oncology

journal homepage: www.thegreenjournal.com

Original Article

RBE-weighted dose in carbon ion therapy for ACC patients: Impact of the RBE model translation on treatment outcomes

Silvia Molinelli [a,*], Maria Bonora [a], Giuseppe Magro [a], Silvia Casale [b], Jon Espen Dale [c], Piero Fossati [d], Azusa Hasegawa [e], Alfredo Mirandola [a], Sara Ronchi [a], Stefania Russo [a], Lorenzo Preda [a,f], Francesca Valvo [a], Roberto Orecchia [a,g], Mario Ciocca [a], Barbara Vischioni [a]

[a] Clinical Department, National Center for Oncological Hadrontherapy (CNAO); [b] Department of Diagnostic Medicine, Institute of Radiology, IRCCS San Matteo University Hospital Foundation, Pavia, Italy; [c] Department of Oncology and Medical Physics, Haukeland University Hospital, Bergen, Norway; [d] MedAustron Ion Therapy Center, Wiener Neustadt, Austria; [e] Osaka Heavy Ion Therapy Center, Osaka, Japan; [f] Department of Clinical-Surgical, Diagnostic and Paediatric Sciences, University of Pavia; and [g] European Institute of Oncology, Milan, Italy

ARTICLE INFO

Article history:
Received 17 May 2019
Received in revised form 23 July 2019
Accepted 26 August 2019
Available online 12 September 2019

Keywords:
Carbon ion therapy
Relative biological effectiveness modeling
Adenoid cystic carcinoma

ABSTRACT

Purpose/objective: The purpose of this study is to assess the impact of the conversion scheme for relative biological effectiveness (RBE)-weighted dose (D_{RBE}), implemented at our center, on treatment outcomes of adenoid cystic carcinoma (ACC) patients.

Material/methods: Treatment plans of 78 ACC patients, optimized with the Local Effect Model (LEM), were recalculated with the modified Microdosimetric Kinetic Model (mMKM). D_{RBE} to 95%, 50% and 2% ($D_{V\%}$) of the clinical target volume (CTV), were selected as relevant parameters to compare LEM and mMKM D_{RBE}. The pattern of failure of ACC treatments was analyzed in relation to uncertainties involved in the D_{RBE} translation methodology.

Results: mMKM recalculations of LEM plans, optimized to a prescription dose of 68.8 Gy(RBE), showed a $D_{50\%}$ 8% higher, on average, than the expected value (60.8 Gy(RBE)), closer to the most frequently used mMKM prescription D_{RBE} (64 Gy(RBE)). $D_{95\%}$ and $D_{2\%}$ deviations, with respect to the optimization goals in the two RBE systems, increased of 0.5% and 14.2%, respectively, due to the steeper mMKM RBE variation along the beam path. Local recurrences were mainly (63%) reported in areas where CTV coverage was not satisfactory in the original LEM plan and the mMKM analysis showed that OARs constraints were too conservative.

Conclusion: No case of local recurrence could be explained by inadequate mMKM target coverage that was not already present in the LEM plan. New constraints have been defined for optic pathways and brainstem to improve target coverage with no expected increase in tissue complications.

Carbon ion radiation therapy (CIRT) combines radiobiological and physical properties, with respect to other sources of external beam radiation therapy, that have a potential advantage for eradication of radioresistant tumours [1]. The high linear energy transfer (LET) of carbon ions provides a higher relative biological effectiveness (RBE) and a lower oxygen enhancement ratio, while physical properties as the sharp dose falloff in the Bragg peak region and minimal lateral scattering allow the delivery of highly conformal dose distributions [2]. Clinical studies conducted at the National Institute of Radiological Sciences (NIRS, Chiba, Japan) and at the Heidelberg Ion Therapy center (HIT, Heidelberg, Germany) reported favourable outcomes for patients with radioresistant head and neck tumours such as adenoid cystic carcinoma (ACC) treated with CIRT [3–8]. The National center for oncological hadrontherapy (CNAO, Pavia, Italy) started treatments with carbon ions in November 2012 [9] and a total of 1385 patients have been treated to date. CIRT protocols were defined based on pre-clinical studies [10] conducted with the aim of taking advantage of the long term NIRS experience in terms of tumor local control and tissue toxicity. It is well known that carbon ion (RBE)-weighted dose (D_{RBE}) strongly depends on the RBE model implemented in the treatment planning system (TPS). Practically, the same absorbed dose (D_{abs}) generates different D_{RBE} distributions depending on the biological model applied and viceversa. The extent of variation has been previously quantified for phantom and patient cases [10–13]. Three models are currently in clinical use for CIRT: the local effect model (LEM, version I) [14,15] the modified microdosimetric kinetic model (mMKM) [16] and the semi-empirical mixed

* Corresponding author at: Clinical Department, National Center for Oncological Hadrontherapy, Strada Campeggi 53, 27100 Pavia, Italy.
E-mail address: molinelli@cnao.it (S. Molinell.

https://doi.org/10.1016/j.radonc.2019.08.022
0167-8140/

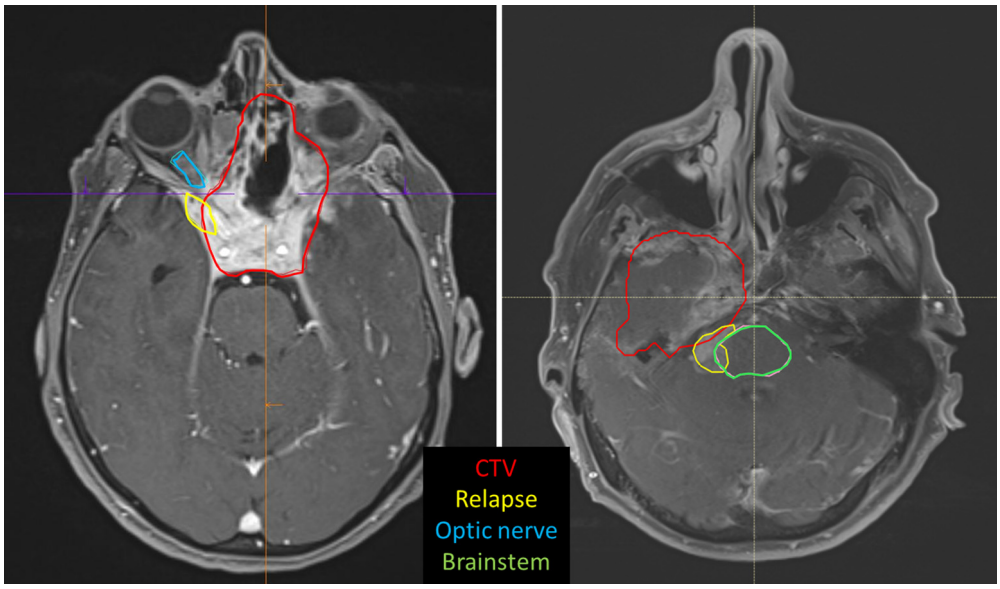

Fig. 1. Axial MR projection of two ACC patients showing the CTV (red line), relapse (yellow line), optic nerve (blue line) and brainstem (green line) contours. (For interpretation of the references to colour in this figure legend, the reader is referred to the web version of this article.)

beam model adopted in japanese CIRT centers for passive scattering treatments [17,18]. The latter two have been validated for consistency [16] and they will therefore be considered as a unique RBE system in the following (mMKM). Fossati et al. described in detail the clinical approach followed at CNAO for definition of LEM-based prescription doses ($D_{RBE|LEM}$), which aimed at reproducing NIRS clinical results (mMKM-based; $D_{RBE|MKM}$) [10]. To translate $D_{RBE|MKM}$ into the $D_{RBE|LEM}$ prescription dose levels that delivers the closest D_{abs}, we adopted conversion factors ranging from 1.04 to 1.15, while prudentially no correction was applied to organ at risk (OAR) constraints. Prescription dose conversion factors increase as the mMKM prescribed dose per fraction decreases. For tumors such as prostate adenocarcinoma, a factor of 1.15 is applied to convert the prescription D_{RBE} from 3.6 Gy(RBE) to 4.15 Gy(RBE) per fraction, while 1.04 is applied to pancreas adenocarcinoma prescription D_{RBE}, to convert it from 4.6 Gy(RBE) to 4.8 Gy(RBE) per fraction. There are two main weak points in this approach. First, target dose homogeneity (taking mMKM as a reference) is not preserved, because at the same dose level and for the same spread out Bragg peak (SOBP) size, the mMKM predicts a more rapid increase in RBE as a function of LET (depth), compared to LEM. Conversion factors minimize deviations in D_{abs}, corresponding to the prescription D_{RBE} in the two systems, at the SOBP center. When translating plans from LEM to mMKM, the approach described guarantees an accurate prediction of the median target D_{RBE} ($D_{50\%}$) [12], while unavoidably generating hot spots in the distal part and cold spots in the proximal part of the beam path, respectively. Therefore, plan evaluation criteria such as D_{RBE} to 95% ($D_{95\%}$) and 2% ($D_{2\%}$) of the clinical target volume (CTV) will show a larger variation than $D_{50\%}$. The second weak point concerns the conservative approach to healthy tissue sparing with no correction applied to OARs constraints, attributable to a safety measure undertaken at the beginning of clinical activity with CIRT. Indeed, it has been shown that D_{RBE} differences between the two systems can be higher outside than inside the target volume, with deviations as high as 60% in the beam entrance region [13]. The $D_{RBE|LEM}$ overestimation outside the target volume is markedly reduced when LEM version IV is used for RBE calculation [13,19]. However, to date this model version has never been adopted in clinical practice.

The aim of this work is to evaluate the clinical implications of the described approach in terms of local control (LC) for ACC patients treated at CNAO. In particular, we first verified the accuracy of the dose conversion factor and its dependence on the prescription dose level. Then we investigated statistical correlation of D_{RBE} deviations with target volume, beam number and configuration. Afterwards, we analyzed the pattern of failure of patient presenting a relapse at follow-up to evaluate the impact on loss of LC of target $D_{RBE|MKM}$ inhomogeneity and OARs sparing. A detailed evaluation of ACC carbon ion treatment outcomes at CNAO is out of the scope of this work and will be discussed in a clinical manuscript in preparation.

Materials and methods

Patient selection and treatment characteristics

At the time of definition of the CNAO clinical protocols for CIRT treatment, the reference NIRS prescription $D_{RBE|MKM}$ for ACC patients ranged form 57.6 to 64 Gy(RBE) in 16 fractions [3]. With the aim of reproducing the mean $D_{RBE|MKM}$ value of 60.8 Gy(RBE), we defined a $D_{RBE|LEM}$ value of 68.8 Gy(RBE) in 16 fractions, prescribed to the median CTV dose [12]. Dose constraints to the optic pathways were $D_{1\%} < 40$ Gy(RBE) and $D_{20\%} < 28$ Gy(RBE) [20] and for the brainstem, $D_{1\%} < 30$ Gy(RBE). Patients were followed every three months with clinical examination and magnetic resonance imaging for the first two years after treatment completion; every six months until the fifth year and yearly thereafter. For evaluation of LC, in September 2018 we reviewed 128 patients, consecutively treated with curative intent from March 2013 to September 2016 in the framework of the prospective protocol (CNAO S9/2012/C), with a median follow-up of 36 months (range 4–64 months). Within this patient set, 30 patients (23%) developed a relapse during follow up. For data analysis, a control group of 38 patients, with similar mean target volume and follow-up time, was selected among the S9 protocol. Overall, CTV volume ranged from 2.1 cc to 403.4 cc (mean 119.5 cc; median 89.0 cc). Mean target volumes were (125 ± 80.7) cc and (106.5 ± 76.1) cc, while median follow up was 34 (range 11–63) and 38 (range 4–64) months, for the control and relapse group respectively. From beginning of 2017 selected patients at risk of major toxicity, due to comorbidity and extension of the primary tumor, are treated with a slightly lower prescription $D_{RBE|LEM}$ of 65.6 Gy(RBE). A small patient sample (n = 10) from this

latter group was also included to analyse dependence of the dose conversion factor on the prescription dose. All treatment plans were optimized with Syngo PT TPS (Siemens AG Healthcare, Erlangen, Germany) based on the LEM model. Three beams were used for 17 patients (2 lateral opposed beams and one beam from the vertex), while 51 patients were treated with 2 beams with a beam separation angle of ≈ 45° (34), 90° (15), 180° (12).

Data analysis

Patient CT, structure set, RTPlan and RTdose files were exported for recalculation with Raystation V6.99 (Raysearch, Stockolm, Sweden), a TPS research version able to support both LEM and mMKM D_{RBE}. All plans were recalculated with Raystation, using a carbon ion beam model commissioned on the CNAO beam line. D_{RBE} distributions were first calculated with LEM and compared to the original Syngo plan to guarantee dosimetric agreement (results not reported). Subsequently, mMKM was applied to the same D_{abs} distribution to obtain $D_{RBE|MKM}$. Data analysis was focused on CTV dose volume points ($D_{v\%}$) comparison between the two RBE frameworks. For each patient, CTV $D_{95\%}$, $D_{50\%}$ and $D_{2\%}$ were collected for $D_{RBE|LEM}$ and $D_{RBE|MKM}$ distributions as indicators of low, prescription and high dose levels, respectively. Target coverage constraints adopted for plan optimization were considered as D_{RBE} goals: CTV $D_{95\%} > 95\%$ and CTV $D_{2\%} < 110\%$ of the prescription dose, respectively. We analysed average percentage $D_{v\%}$ variations ($\Delta D_{v\%}$) for LEM and mMKM plans, with respect to the aforementioned dosimetric goals, for the three patient groups described in the previous paragraph. A *t*-test was conducted among the 68.8 Gy(RBE) sample to assess statistical differences in mMKM average $\Delta D_{v\%}$ between the relapse and control group. A significance level of 5% (*p*-value <0.05) was fixed under the null hypothesis of no difference in $D_{v\%}$. Moreover, volume and beam configuration dependence of mMKM $\Delta D_{v\%}$ for the same sample were evaluated with the same statistical procedure against the null hypothesis of no dependency. The statistical analysis was conducted with Matlab (Matlab® R2017b, The MathWorks Inc., Massachusetts, USA).

For the 30 patients with relapse, two medical doctors independently reviewed CTV contours for adequacy. A radiologist contoured the recurrent tumor on the follow-up MR, previously registered with the planning CT scan. Relapse location was evaluated by one medical physicist and two medical doctors, with respect to CTV and OARs (Fig. 1) contoured on pre-treatment MR and both D_{RBE} distributions (LEM and mMKM). Patients with CTV delineation not adhering to the internal CNAO contouring guidelines [21] were excluded from the subsequent analysis. For the remaining patient group, the relapse contour was classified as in-field (including field edge) or out-of-field. For the in-field group, the relapse position in the $D_{RBE|LEM}$ distribution was evaluated to sort recurrences appearing in a low (or acceptable) $D_{RBE|LEM}$ region (($D_{95\%} < (\geq)$ 95% of the prescription dose). The potential cause of underdosage was investigated case by case. For well covered volumes, relapses were grouped as originating in a low $D_{RBE|MKM}$ region ($D_{95\%} < 95\%$ of the goal prescription dose), due to target dose inhomogeneity arising after dose translation, or in a well covered $D_{RBE|MKM}$ area ($D_{95\%} \geq 95\%$).

Results

Table 1 shows average DVH points (±1 standard deviation), together with $\Delta D_{v\%}$ with respect to the goals, among the patients analysed, grouped by prescription dose level first and LC outcomes for the 68.8 Gy(RBE) sample. LEM plans for the 68.8 Gy(RBE) group could not respect the $D_{95\%}$ constraint on average. Cold spots minimally worsen in mMKM recalculations (4.0% vs 3.5%). The LEM

Table 1
Average (±1standard deviation) CTV DVH points $D_{v\%}$ (v = 95, 50, 2) over LEM-optimized and mMKM-recalculated plans grouped according to the prescription dose. For the 68.8 Gy(RBE) dose level, average values are reported for the relapsed and control groups separately. The $D_{RBE|MKM}$ defined goals, taken as a reference, are presented in bold. For each group, the variation between $D_{RBE|LEM}$ and $D_{RBE|MKM}$ values with respect to the goals ($\Delta D_{v\%}$) is presented. The number of patients included in each group is reported in brackets together with the subset receiving a plan optimized with a 2 beam configuration at ≈45° separation angle.

				68.8 Gy(RBE)										65.6 Gy(RBE)			
				All (68) 45° (28)				Relapsed (30) 45° (9)				Control (38) 45° (18)		(10) 45° (6)			
CTV	LEM 68.8 GOALS Gy (RBE)	LEM 65.6 GOALS Gy (RBE)	MKM GOALS Gy(RBE)	LEM Gy (RBE)	$\Delta D_{v\%}$ (%)	MKM Gy (RBE)	$\Delta D_{v\%}$ (%)	LEM Gy (RBE)	$\Delta D_{v\%}$ (%)	MKM Gy (RBE)	$\Delta D_{v\%}$ (%)	LEM Gy (RBE)	$\Delta D_{v\%}$ (%)	MKM Gy (RBE)	$\Delta D_{v\%}$ (%)	LEM Gy (RBE)	$\Delta D_{v\%}$ (%)	MKM Gy (RBE)	$\Delta D_{v\%}$ (%)
$D_{95\%}$	65.4	62.3	**57.8**	63.1 ± 4.0	−3.5	55.5 ± 5.8	−4.0	62.0 ± 4.9	−5.2	54.2 ± 7.1	−6.2	63.9 ± 3.0	−2.3	56.4 ± 4.4	−2.4	62.6 ± 2.1	0.5	54.4 ± 4.1	−5.9
$D_{50\%}$	68.8	65.6	**60.8**	69.5 ± 1.6	1.0	65.6 ± 3.1	7.9	69.1 ± 2.1	0.4	64.7 ± 4	6.4	69.9 ± 0.9	1.6	66.4 ± 2.2	9.2	66.2 ± 0.9	0.9	61.0 ± 2.1	0.3
$D_{2\%}$	75.7	72.2	**66.9**	73.1 ± 1.5	−3.4	74.1 ± 3.2	10.8	72.7 ± 1.2	−4.0	73.1 ± 3.3	9.2	73.5 ± 1.5	−2.9	74.8 ± 3.0	11.8	68.7 ± 1.5	−4.8	68.4 ± 2.2	2.2

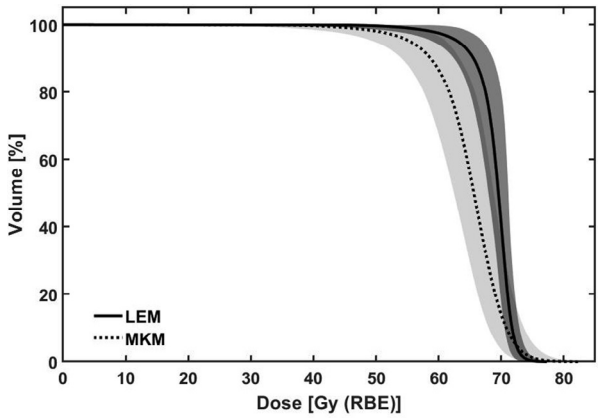

Fig. 2. Average CTV DVH for the 68.8 Gy(RBE) group for the optimized $D_{RBE|LEM}$ (solid line) and recalculated $D_{RBE|MKM}$ (dotted line) distributions. DVH bands represent ± 1 standard deviation.

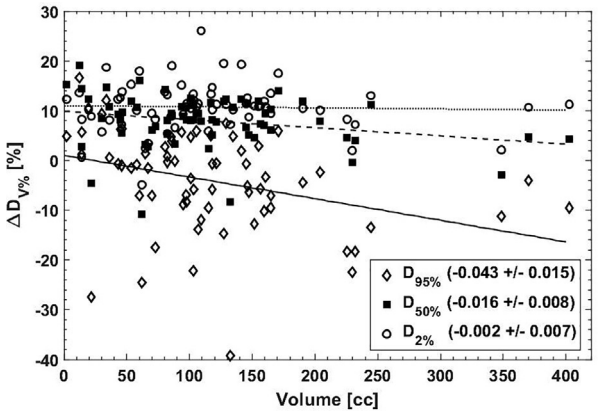

Fig. 3. For each patient of the 68.8 Gy(RBE) group, $D_{RBE|MKM}$ percentage variation with respect to the goal ($\Delta D_{V\%}$) as a function of CTV volume, together with the corresponding trend line, of $D_{95\%}$ (diamonds – solid line), $D_{50\%}$ (squares – dashed line) and $D_{2\%}$ (circles – dotted line). Slopes +/− one standard deviation are reported in the legend.

$D_{95\%}$ goal was respected at 65.5 Gy(RBE) but significantly worsen in the mMKM recalculation (-5.9% vs 0.5%). On the other hand, the $D_{2\%}$ goal could always be respected in LEM plans while showed substantially higher mMKM hot spots (10.8% vs −3.4%). The mMKM $D_{50\%}$ for the 68.8 Gy(RBE) group was closer to the highest NIRS prescription dose value of 64 Gy(RBE), recently reported as the most frequently used for ACC treatments in Japan [7]. The lower LEM prescription dose level (65.6 Gy(RBE)) well matched $D_{RBE|MKM}$ with the initial goal of 60.8 Gy(RBE). Differences in mMKM $\Delta D_{V\%}$ between the relapsed and control group were statistically significant for $D_{50\%}$ (p-value: 0.016) and $D_{2\%}$ (p-value: 0.016), with a very low absolute $D_{v\%}$ difference (<2 Gy(RBE)) between the two groups in both cases.

In Fig. 2 we plotted the average CTV DVHs for the optimized $D_{RBE|LEM}$ and recalculated $D_{RBE|MKM}$ distributions, over all patients treated to 68.8 Gy(RBE). As expected, when mMKM acts on a LEM-optimized D_{abs}, D_{RBE} becomes more inhomogeneous, due to the steeper RBE increase as a function of LET predicted by the mMKM model. The corresponding plot for the small 65.6 Gy(RBE) patient group is presented in Figure Supplementary figure 1 Appendix A, Fig. A1. The $\Delta D_{V\%}$ behaviour as a function of target volume is plotted in Fig. 3 for all 68.8 Gy(RBE) patients, together with a linear fit for qualitative visualization of the trend of variation. The variation was statistically significant for $\Delta D_{95\%}$ (p-value: 0.004) and $\Delta D_{50\%}$ (p-value: 0.041). For what concerns beam configuration, no significant difference was found between average $\Delta D_{V\%}$ as calculated over patients grouped according to the number of beams used for planning. In the mMKM-recalculated plan hot spots are expected in the distal part of the beam path, where $D_{abs|LEM}$ is higher than it should be to generate a homogeneous $D_{RBE|MKM}$. Therefore, the worst case scenario happens when 2 fields are used with a beam separation of ≈45° and a consequently substantial overlap of the distal regions. In the 2 fields sample, a statistically significant increase in $D_{50\%}$ (2.0 Gy(RBE); p-value: 0.029) and $D_{2\%}$ (1.9 Gy(RBE); p-value: 0.029) was found for the 45° group, when compared to the 90° and 180° merged together. The number of treatment plans optimized with a ≈45° configuration is reported in Table 1 for each patient group.

Results of the pattern of failure analysis of the relapsed group are presented in Fig. 4. The number of patients for each category is reported in brackets. In 2% (3/128) of the cases, treated between May 2013 and August 2014, target delineation was not adhering to the internal contouring guidelines. Of the remaining, 85% (23/27) relapsed in-field and in 70% of the cases (19/27) the CTV received a low $D_{95\%}$ in the original LEM plan. In this latter group, CTV underdosage was always directly correlated to OARs sparing, mainly involving optic pathways (11) and brainstem (5). For the last 4 patients with a well covered CTV in the original LEM plan, no relation was found between in-field relapses and the resulting negative mMKM $\Delta D_{95\%}$.

Discussion

For the prescription $D_{RBE|LEM}$ level of 68.8 Gy(RBE), the resulting average $D_{RBE|MKM}$ median target dose ((65.6 ± 3.1) Gy(RBE)) was closer to the highest $D_{RBE|MKM}$ prescription level of 64 Gy(RBE), than the expected $D_{RBE|MKM}$ value of 60.8 Gy(RBE). In the most recently published multicenter study on ACC from the Japan Carbon-Ion Radiation Oncology Study Group, 64 Gy(RBE) has been reported as median total dose and most frequently prescribed dose for ACC patients (134/289) [7]. Assuming this value as the new goal for the 68.8 Gy(RBE) group, mMKM $\Delta D_{95\%}$ in Table 1 would increase from −4.0% to −8.7% and $\Delta D_{2\%}$ would decrease from 10.8% to 5.2%. No relapse was located in a well covered area, in the original LEM plan, corresponding to an underdosed mMKM region resulting from RBE translation. The patient sample in this latter group is very small (4), but this conclusion is indirectly supported by the fact that no significant difference was found in mMKM $\Delta D_{95\%}$ between relapse and control groups. Since beginning of 2017, patients at high risk of toxicity receive a prescription dose to 65.6 Gy(RBE), with the result of a median target dose very close to the 60.8 Gy(RBE) goal and only small regions of target overdose ($\Delta D_{2\%}$ = 2.2%). In addition, for all patients a stricter optimization constraint was introduced on CTV $D_{1\%}$ < 103% of the prescribed $D_{RBE|LEM}$ to implicitly limit high $D_{RBE|MKM}$ values. Conversion factors were estimated on simple target geometries in water with an expected increase of D_{RBE} deviations as a function of the target volume [10]. Consequently, LEM- and mMKM-based D_{abs} match at the SOBP center for average size targets, while as the CTV size increases, absorbed dose profiles intersect at larger depths along the beam path thus broadening the proximal area where $D_{abs|LEM}$ and $D_{abs|MKM}$ diverge, represented by CTV $D_{50\%}$ and $D_{95\%}$. Absolute $D_{RBE|MKM}$ differences determined by the beam configuration were very small, even in the worst case scenario of 2 beams separated by ≈45°, maximizing the beam distal part overlap. It is anyhow very difficult to modify the number of fields and fields configuration for most of our patient cases, while concomitantly taking into account beam angle limitations, due to the absence of a gantry, and optimization requirements related to OARs sparing and plan robustness.

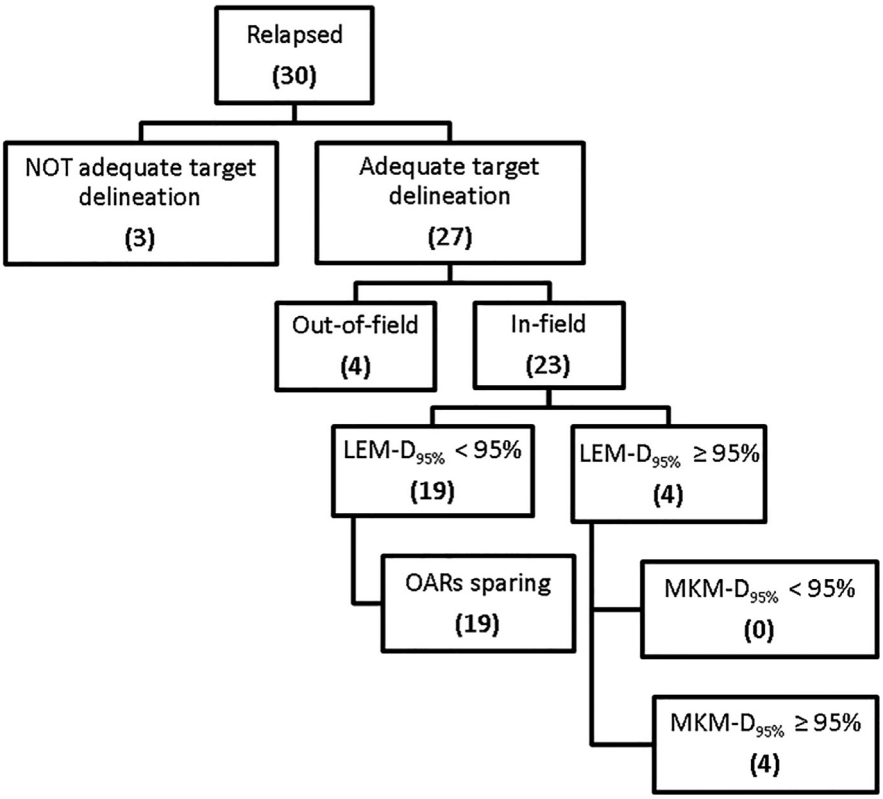

Fig. 4. Patterns of failure of ACC treatments. Patients are ranked according to: adequacy of target delineation to the internal contouring guidelines; location of the relapse defined as in-field or out-of-field; compliance with the CTV coverage goal on $D_{95\%}$ in the original LEM plan; cause of CTV underdosage; compliance with the CTV coverage goal on $D_{95\%}$ in the recalculated mMKM plan. The number of patients included in each category is reported in brackets.

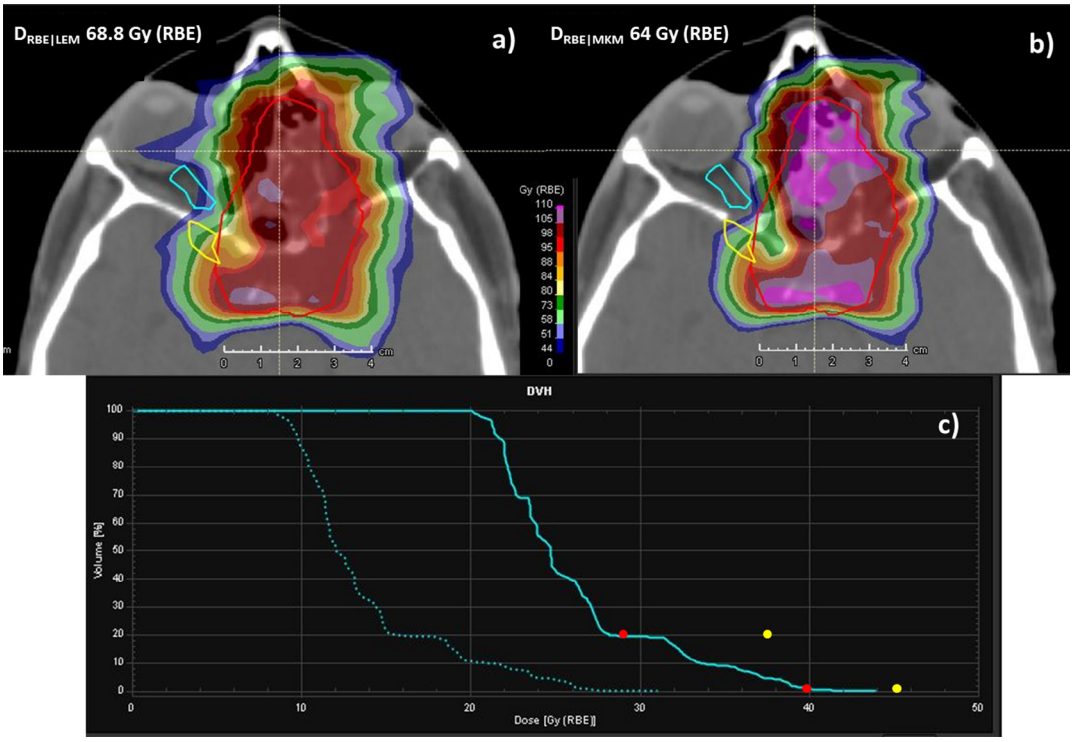

Fig. 5. a) Axial D_{RBE} distribution of a LEM-optimized plan to 68.8 Gy(RBE). b) Axial D_{RBE} distribution of the corresponding mMKM-recalculated plan (doses are normalized to 64 Gy(RBE)), showing the appearance of D_{RBE} hot and cold spots. The CTV contour is plotted in red, the optic nerve in light blue and the relapse in yellow. c) Optic nerve DVHs corresponding to LEM (solid lines) and mMKM (dotted lines) computations. The red dots point to the mMKM-defined NIRS constraint, while yellow dots indicate the new constraints implemented at CNAO. (For interpretation of the references to colour in this figure legend, the reader is referred to the web version of this article.)

For the majority of ACC patients presenting a relapse, the pre-treatment target volume was found underdosed due to OARs sparing. In particular, 11 and 5 patients relapsed close to the optic pathways and brainstem, respectively. To date, no unexpected visual and brainstem toxicities have been reported for any patients treated at CNAO. Fig. 5 presents a case of relapse located in the underdosed CTV region close to the optic nerve. As shown in Fig. 5c), the mMKM-recalculated optic nerve DVH lies well below the applied constraints (red dots), unveiling a wide margin for D_{RBE} increase. As already discussed, D_{RBE} differences outside the target volume can be significantly higher than in the SOBP region. In addition, as D_{RBE} decreases the deviation between the two RBE systems increases making the dose fall-off from the CTV to the optic nerve steeper in the mMKM-recalculated plan (Fig. 5b)) than in the original LEM-weighted plan (Fig. 5a)). Since October 2018 the optic nerve and chiasm constraint have been increased to $D_{1\%} < 45$ Gy (RBE) and $D_{20\%} < 37$ Gy(RBE) (Fig. 5c)) and brainstem constraints to $D_{0.7cc} < 38$ Gy(RBE) and $D_{0.1cc} < 46$ Gy(RBE), respectively. Due to the relatively constant brainstem size in the patient population, the newly adopted constraints approximately correspond to a $D_{\approx 1\%} < 40$ Gy(RBE). These data are the result of a retrospective study involving $D_{RBE|LEM}$ and $D_{RBE|MKM}$ comparison and NTCP evaluation for 38 head and neck (H&N) patients [22].

Sources of uncertainty to be accounted for mainly relate to the use of different TPS (and calculation algorithms) for clinical treatment at CNAO and NIRS and, in this specific project, for data analysis. In Molinelli et al, the use of different algorithms for dose computation determined an average D_{abs} variation in the target region of about 2.5% for H&N patients [12]. Different approaches to mixed radiation beam modeling may cause discrepancies in D_{RBE} distributions depending on the fragmentation spectra description accuracy and on the RBE model used [23]. It has been shown that, for a H&N case treated at dose levels discussed here, a local D_{abs} difference of 5% at the isocenter would translate in a lower local D_{RBE} difference of 2% [12]. On the other side, relative deviations between $D_{RBE|LEM}$ and $D_{RBE|MKM}$ values reported in Table 1 are not affected by the aforementioned uncertainties, since they have been calculated with the same TPS.

At 5 years from the beginning of CIRT clinical activity we completed the dosimetric analysis of a subset of ACC treatments plans in relation to the dose conversion approach applied. The process described here was of fundamental importance in our clinical practice to improve treatment quality based on the corrective actions undertaken. New optimization goals and OAR constraints currently in clinical use have been summarized in Appendix A, Table A1. A clinical evaluation of treatment outcomes in terms of CIRT toxicity and efficacy for all treated ACC patients is currently undergoing. Following the same method presented, we are evaluating dose conversion factors and $D_{RBE|MKM}$ distributions for other diseases, such as skull-base and sacral chordoma, pancreatic and prostate adenocarcinoma. Dose constraints to the gastro-intestinal district (e.g.: rectum, sigmoideum, duodenum, stomach) will also be optimized in terms of $D_{RBE|LEM}$ to minimize the existing gap between nominal and recalculated $D_{RBE|MKM}$.

The conversion factor applied to define a LEM-based prescription dose agreed well with the most frequently adopted dose level in Japanese CIRT centers. Target $D_{RBE|MKM}$ inhomogeneity, specifically generated by the D_{RBE} conversion, was not correlated to loss of LC in the patient group analyzed. D_{RBE} deviations between LEM-optimized and mMKM-recalculated plans were significantly higher in regions where steep dose gradients enabled OARs sparing, than in the target region. New constraints are currently applied for optic pathways and brainstem at CNAO to improve target coverage with no expected increase in tissue complications.

Declaration of Competing Interest

The authors declare that they have no known competing financial interests or personal relationships that could have appeared to influence the work reported in this paper.

Acknowledgement

The authors would like to thank Erik Traneus and the RaySearch Carbon ion group for providing the Raystation V6.99 research TPS version.

Appendix A. Supplementary data

Supplementary data to this article can be found online at https://doi.org/10.1016/j.radonc.2019.08.022.

References

[1] Kamada T, Tsujii H, Blakely EA, Debus J, De Neve W, Durante M, et al. Carbon ion radiotherapy in Japan: an assessment of 20 years of clinical experience. Lancet Oncol 2015;16:e93–e100.
[2] Amaldi U, Kraft G. Radiotherapy with beams of carbon ions. Rep Prog Phys 2005;68:1861–82.
[3] Mizoe JE, Hasegawa A, Jingu K, Takagi R, Bessyo H, Morikawa T, et al. Results of carbon ion radiotherapy for head and neck cancer. Radiother Oncol 2012;103:32–7.
[4] Tsujii H, Kamada T. A review of update clinical results of carbon ion radiotherapy. Jpn J Clin Oncol 2012;42:670–85.
[5] Takagi M, Demizu Y, Hashimoto N, Mima M, Terashima K, Fujii O, et al. Treatment outcomes of particle radiotherapy using protons or carbon ions as a single-modality therapy for adenoid cystic carcinoma of the head and neck. Radiother Oncol 2014;113:364–70.
[6] Jensen AD, Nikoghosyan AV, Lossner K, Haberer T, Jäkel O, Münter MW, et al. COSMIC: a regimen of intensity modulated radiation therapy plus dose-escalated, raster-scanned carbon ion boost for malignant salivary gland tumors: results of the prospective phase 2 trial. Int J Radiat Oncol Biol Phys 2015;93:37–46.
[7] Sulaiman NS, Demizu Y, Koto M, Saitoh J, Suefuji H, Tsuji H, et al. Multicenter study of carbon-ion radiation therapy for adenoid cystic carcinoma of the head and neck: subanalysis of the japan carbon-ion radiation oncology study group (J-CROS) study (1402 HN). Int J Radiat Oncol Biol Phys 2018;100:639–46.
[8] Akbaba S, Ahmed D, Lang K, Held T, Mattke M, Hoerner-Rieber J, et al. Results of a combination treatment with intensity modulated radiotherapy and active raster-scanning carbon ion boost for adenoid cystic carcinoma of the minor salivary glands of the nasopharynx. Oral Oncol 2019;91. p. 39–46..
[9] Rossi S. The National Centre for Oncological Hadrontherapy (CNAO): Status and perspectives. Phys Med 2015;31:333–51.
[10] Fossati P, Molinelli S, Matsufuji N, Ciocca M, Mirandola A, Mairani A, et al. Dose prescription in carbon ion radiotherapy: a planning study to compare NIRS and LEM approaches with a clinically-oriented strategy. Phys Med Biol 2012;57:7543–54.
[11] Steinstrater O, Grün R, Scholz U, Friedrich T, Durante M, Scholz M. Mapping of RBE-weighted doses between HIMAC- and LEM-Based treatment planning systems for carbon ion therapy. Int J Radiat Oncol Biol Phys 2012;84:854–60.
[12] Molinelli S, Magro G, Mairani A, Matsufuji N, Kanematsu N, Mirandola A, et al. Dose prescription in carbon ion radiotherapy: How to compare two different RBE-weighted dose calculation systems. Radiother Oncol 2016;120:307–12.
[13] Magro G, Dahle TJ, Molinelli S, Ciocca M, Fossati P, Ferrari A, et al. The FLUKA Monte Carlo code coupled with the NIRS approach for clinical dose calculations in carbon ion therapy. Phys Med Biol 2017.
[14] Scholz M, Kellerer A, Kraft-Weyrather W, Kraft G. Computation of cell survival in heavy ion beams for therapy. Radiat Environ Biophys 1997;36:59–66.
[15] Kramer M, Scholz M. Treatment planning for heavy-ion radiotherapy: calculation and optimization of biologically effective dose. Phys Med Biol 2000;45:3319–30.
[16] Inaniwa T, Kanematsu N, Matsufuji N, Kanai T, Shirai T, Noda K, et al. Reformulation of a clinical-dose system for carbon-ion radiotherapy treatment planning at the National Institute of Radiological Sciences, Japan. Phys Med Biol 2015;60:3271–86.
[17] Kanai T, Furusawa Y, Fukutsu K, Itsukaichi H, Eguchi-Kasai K, Ohara H. Irradiation of mixed beam and design of spread-out Bragg peak for heavy-ion radiotherapy. Radiat Res 1997;147:78–85.
[18] Kanai T, Endo M, Minohara S, Miyahara N, Koyama-ito H, Tomura H, et al. Biophysical characteristics of HIMAC clinical irradiation system for heavy-ion radiation therapy. Int J Radiat Oncol Biol Phys 1999;44:201–10.
[19] Grün R, Friedrich T, Elsässer T, Krämer M, Zink K, Karger CP, et al. Impact of enhancements in the local effect model (LEM) on the predicted RBE-weighted target dose distribution in carbon ion therapy. Phys Med Biol 2012;57:7261–74.

[20] Hasegawa A, Mizoe JE, Mizota A, Tsujii H. Outcomes of visual acuity in carbon ion radiotherapy: analysis of dose-volume histograms and prognostic factors. Int J Radiat Oncol Biol Phys 2006;64:396–401.
[21] Fossati P, Mizoe JE, Vitolo V, Iannalfi A, Hasegawa A, Kamada T et al. Imaging and contouring procedures for head and neck adenoid cystic carcinoma at the National Institute of Radiological Science (NIRS). ULICE: Project co-funded by the European Commission within the FP7 (2007–2013). https://espace.cern.ch/ULICE-results/Shared%20Documents/NA_10.3_public.pdf.
[22] Dale JE, Molinelli S, Vitolo V, Vischioni B, Bonora M, Magro G, et al. Optic nerve constraints for carbon ion RT at CNAO – reporting and relating outcome to European and Japanese RBE. Radiother Oncol 2019;140:175–81.
[23] Böhlen T, Cerutti F, Chin M, et al. The FLUKA code: developments and challenges for high energy and medical applications. Nucl Data Sheets 2014;120:211–4.